Micro Gas Turbines – A Short Survey of Design Problems

R.A. Van den Braembussche
von Kármán Institute for Fluid Dynamics
Waterloose steenweg, 72
B-1640, Rhode-St-Genèse
BELGIUM

vdb@vki.ac.be

INTRODUCTION

Micro gas turbines have experienced a growing interest during the last decade. Their large energy density (Whr/kg) makes them attractive for portable power units as well as for propulsion of small airplanes (UAV). They are also of interest for distributed power generation in applications where heat and power generation can be combined. The need for high performance in both applications is at the origin of a worldwide interest and research on micro gas turbines and the motivation for the present lecture series.

Scaling is a common technique to define larger or smaller geometries with similar characteristics. However a simple scaling of a high performance large gas turbine will not result in a good micro gas turbine. The main factors perturbing such a scaling are:

- *The large change in Reynolds number.*
- *Massive heat transfer between the hot and cold components (negligible in large machines).*
- *Geometrical restrictions related to material and manufacturing of miniaturized components.*

The purpose of the present lecture is to provide a first insight into the aero-thermal problems of micro gas turbines.

1.0 GAS TURBINE SCALING

1.1 Scaling Model

Conservation of the characteristics of the thermodynamic cycle is a first requirement when scaling a gas turbine. This means the same exchange of the energy between fluid and rotating components but at a smaller mass flow. Hence the enthalpy change in the compressor and turbine should be conserved.

$$\Delta H = \omega^2 . R_2^2 \qquad (1)$$

This provides a relation between RPM and impeller diameter that can easily be satisfied. It also means that the power in each component,

$$\Delta E = Q . \Delta H \qquad (2)$$

and hence the gas turbine power will be proportional to the mass flow Q. Another consequence of maintaining the same velocities and pressures is that the mass flow and power depend on the cross section area and scale with R_2^2.

Van den Braembussche, R.A. (2005) Micro Gas Turbines – A Short Survey of Design Problems. In *Micro Gas Turbines* (pp. 1-1 – 1-18). Educational Notes RTO-EN-AVT-131, Paper 1. Neuilly-sur-Seine, France: RTO. Available from: http://www.rto.nato.int/abstracts.asp.

The main conditions to maintain the level of efficiency of compressors and turbines is the conservation of velocity triangles, Reynolds number and Mach number.

The conservation of Mach number

$$M = \frac{\omega R_2}{\sqrt{\gamma . R_G . T}} \tag{3}$$

does not create problems except for applications with big changes of inlet temperature (T) or gas characteristics (γ, R_G).

Conservation of Reynolds number

$$\mathrm{Re} = \omega . R_2^{\,2} \frac{\rho}{\mu} = \frac{\rho}{\mu} R . \sqrt{\Delta H} \tag{4}$$

conflicts with the conservation of enthalpy change when changing the dimensions of the rotor. A reduction of Reynolds number with decreasing dimensions is unavoidable unless also the viscosity and/or pressure level are modified. The impact of reducing dimensions on compressor performance can be obtained taken from Fig. 1 where the change in efficiency with decreasing mass flow is indicated by the vertical dashed line.

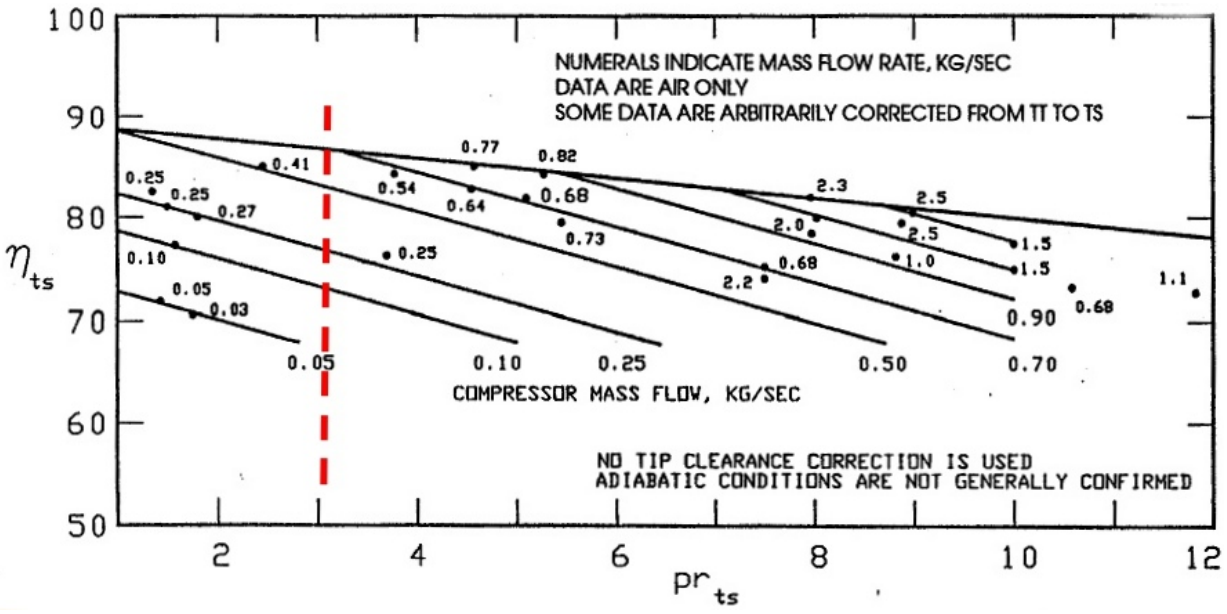

Figure 1: Variation of Compressor Performance with Pressure Ratio and Mass Flow (acc. [1]).

The "Specific speed"

$$Ns = \frac{\omega . \sqrt{Q / \rho}}{\Delta H^{3/4}} \tag{5}$$

is a non-dimensional parameter characterizing the shape of a radial compressor and can be used to estimate the achievable performance. Experience has shown that the highest efficiencies can be obtained

for *Ns* values between .6 and .8 (Fig. 2). Once the enthalpy rise (ΔH) and mass flow (Q) are known it defines the required radial compressor rotational speed. Optimum *Ns* values result in a higher *RPM* for a required mass flow. Designing for a lower *Ns* value allows a lower *RPM* for the same mass flow (or power) but penalizes on efficiency. The higher values of *Ns* lead to *RPM* that may not be reachable (rotor-dynamic and bearing problems) and a lower value of Ns may be a design option to alleviate the bearing problems. The corresponding penalty on efficiency can be obtained from figure 2.

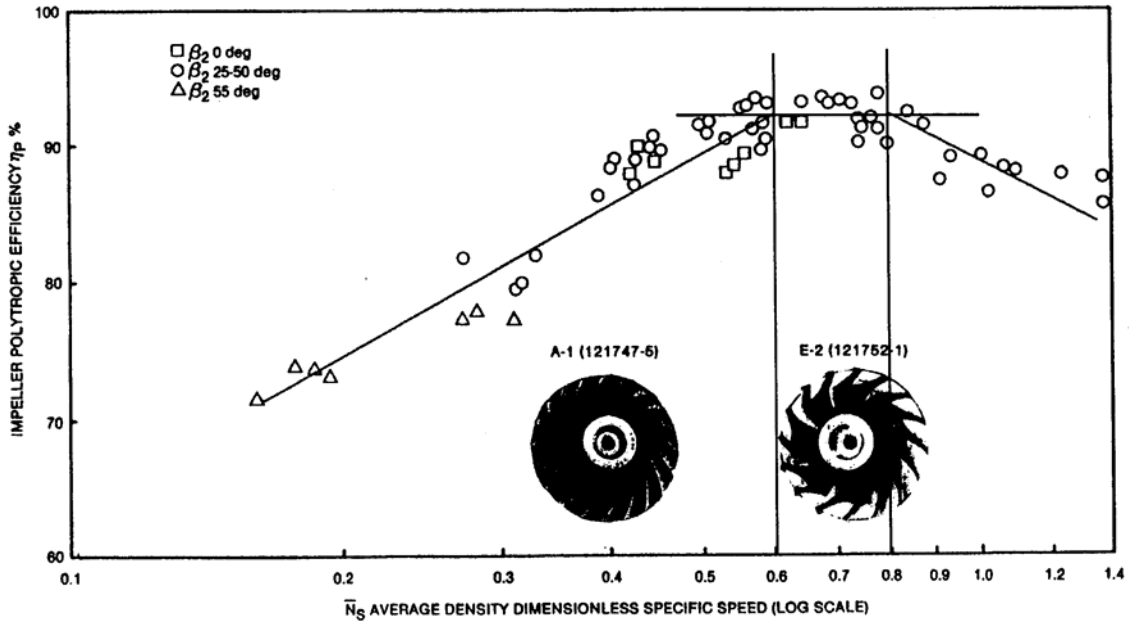

Figure 2: Variation of Achievable Compressor Efficiency with Specific Speed (acc. [2]).

1.2 Performance Predictions

Previous model has been used to predict the compressor performance at different values of impeller *RPM*. The results for high and low values of *Ns* and high and low values of the turbine inlet temperature are summarized in table 1 to 4. Each table shows the variation of the gas turbine characteristics and performance when decreasing the dimensions to finger tip size impellers. The pressure ratio, compressor inlet temperature *T1*, Turbine inlet temperature *Tit*, Specific speed *Ns*, radial compressor slip factor, Turbine efficiency etaT, specific heat *Cp* and Gas constant R_G, at which the calculations are made, are listed in the first rows. Calculations are made for a simple cycle without recuperator.

The compressor efficiency is predicted in two steps. The variation of Eta-Comp (column 8) accounts for the reduction in efficiency with decreasing Reynolds number (Fig. 1). The second step corrects for non-optimum specific speed (Fig. 2). The global result is listed under Eta-C(corr) (column 9).

The turbine efficiency, needed to define the cycle efficiency, is assumed to be independent of the size and fixed at a low (70.%) and high value (80.%). The lower value stands for the worst case when the efficiency is limited by geometrical or manufacturing restrictions (2D instead of 3D impellers).

All predictions are made for pressure ratio = 3. Losses in the piping and combustor are neglected. An increase in ΔH and hence peripheral velocity *U2* is required to compensate for the decrease in compressor efficiency with decreasing size. The important decrease in cycle efficiency with decreasing size, shown on Table 1, illustrates the large impact of compressor and turbine performance at moderate values (1200. ^{o}K) if Tit.

Table 1: Variation of Gas Turbine Performance with Size (Tit = 1200.°K, Ns = .3)

P2/P1	T1	Tit			slip	Ns		etaT	Cp	Rg
3	293	1200			0.9	0.3		0.7	1005	286
RPM	omega	Delta H	U2	R2	Q	Pcomp	Eta-Comp	Eta-C(corr)	(GasTurb)	Eta(cycle)
		(m^2/s^2)	(m/sec)	(m)	(kg/sec)	(kW)			(kW)	
10,000	1047	155115	415	0.39644	5.01379	777.71	0.85	0.7	362.560	0.096
16,000	1676	157363	418	0.24956	2.00124	314.92	0.84	0.69	140.216	0.093
25,000	2618	159677	421	0.16089	0.83786	133.79	0.83	0.68	56.765	0.090
50,000	5236	162060	424	0.08104	0.21417	34.71	0.82	0.67	14.000	0.087
100,000	10472	164516	428	0.04083	0.05476	9.01	0.81	0.66	3.445	0.084
200,000	20944	146730	404	0.01928	0.01153	1.69	0.89	0.74	0.931	0.106
300,000	31416	175130	441	0.01404	0.00668	1.17	0.77	0.62	0.350	0.071
500,000	52360	180967	448	0.00856	0.00253	0.46	0.75	0.6	0.117	0.064
750,000	78540	190492	460	0.00586	0.00121	0.23	0.72	0.57	0.045	0.051
1,000,000	104720	201075	473	0.00451	0.00074	0.15	0.69	0.54	0.020	0.037
2,000,000	209439	212903	486	0.00232	0.00020	0.04	0.66	0.51	0.003	0.021
2,400,000	251327	226209	501	0.00199	0.00015	0.03	0.63	0.48	0.000	0.002

Table 2 illustrates the favorable influence of an increase in specific speed (from .3 to .5) on compressor efficiency. Together with an increase of turbine efficiency (etaT = 80% instead of 70.%) it results in a considerable increase of cycle efficiency. At the smallest dimensions the cycle efficiency has increased to 10% and the gas turbine power has changed from 0. to a small positive value. The mass flow is doubled and the power output is increased with a factor 5. This comparison illustrates the large impact of compressor and turbine efficiency on overall performance and emphasizes the need for optimized components [3].

Table 2: Variation of Gas Turbine Performance with Size (Tit = 1200.°K, Ns = .5)

P2/P1	T1	Tit			slip	Ns		etaT	Cp	Rg
3	293	1200			0.9	0.5		0.8	1005	286
RPM	omega	Delta H	U2	R2	Q	Pcomp	Eta-Comp	Eta-C(corr)	(GasTurb)	Eta(cycle)
		(m^2/s^2)	(m/sec)	(m)	(kg/sec)	(kW)			(kW)	
10,000	1047	135726	388	0.3708	11.3992	1547.169	0.85	0.80	1415.690	0.160
16,000	1676	137444	391	0.2332	4.5376	623.670	0.84	0.79	555.741	0.158
25,000	2618	139206	393	0.1502	1.8945	263.722	0.83	0.78	228.685	0.156
50,000	5236	141014	396	0.0756	0.4829	68.092	0.82	0.77	57.416	0.154
100,000	10472	142869	398	0.0380	0.1231	17.588	0.81	0.76	14.410	0.152
200,000	20944	129262	379	0.0181	0.0265	3.424	0.89	0.84	3.461	0.167
300,000	31416	150806	409	0.0130	0.0148	2.237	0.77	0.72	1.619	0.143
500,000	52360	155115	415	0.0079	0.0056	0.864	0.75	0.70	0.584	0.139
750,000	78540	162060	424	0.0054	0.0026	0.429	0.72	0.67	0.259	0.131
1,000,000	104720	169657	434	0.0041	0.0016	0.270	0.69	0.64	0.144	0.122
2,000,000	209439	178001	445	0.0021	0.0004	0.076	0.66	0.61	0.035	0.112
2,400,000	251327	187208	456	0.0018	0.0003	0.060	0.63	0.58	0.023	0.100

Comparing the results on Table 3 with those on Table 1 illustrates the performance improvements when increasing the *Tit* from 1200 °K to 1500 °K, without any change in compressor and turbine characteristics. It also results in a considerable increase of the power output without change in mass flow.

Table 3: Variation of Gas Turbine Performance with Size (Tit = 1500.°K, Ns = .3)

P2/P1	T1	Tit			slip	Ns		etaT	Cp	Rg
3	293	1500			0.9	0.3		0.7	1005	286
RPM	omega	Delta H	U2	R2	Q	Pcomp	Eta-Comp	Eta-C(corr)	(GasTurb)	Eta(cycle)
		(m^2/s^2)	(m/sec)	(m)	(kg/sec)	(kW)			(kW)	
10,000	1047	155115	415	0.3964	5.0138	777.714	0.85	0.70	647.629	0.122
16,000	1676	157363	418	0.2496	2.0012	314.922	0.84	0.69	254.001	0.120
25,000	2618	159677	421	0.1609	0.8379	133.787	0.83	0.68	104.403	0.118
50,000	5236	162060	424	0.0810	0.2142	34.709	0.82	0.67	26.177	0.116
100,000	10472	164516	428	0.0408	0.0548	9.010	0.81	0.66	6.559	0.114
200,000	20944	146730	404	0.0193	0.0115	1.692	0.89	0.74	1.586	0.129
300,000	31416	175130	441	0.0140	0.0067	1.170	0.77	0.62	0.730	0.105
500,000	52360	180967	448	0.0086	0.0025	0.457	0.75	0.60	0.261	0.100
750,000	78540	190492	460	0.0059	0.0012	0.231	0.72	0.57	0.114	0.092
1,000,000	104720	201075	473	0.0045	0.0007	0.149	0.69	0.54	0.062	0.082
2,000,000	209439	212903	486	0.0023	0.0002	0.043	0.66	0.51	0.014	0.071
2,400,000	251327	226209	501	0.0020	0.0002	0.035	0.63	0.48	0.009	0.059

The best results are obtained with increased Tit and high compressor and turbine performance as shown on Table 4. However it is questionable if this performance level is realistic in small gas turbines where the small dimensions prohibit any blade cooling. Even the use of new materials as SiN will not allow such temperatures and the achievable cycle efficiency may be closer to the one listed in Table 1. The use of these unconventional materials for gas turbine rotors requires new manufacturing techniques and may impose restrictions on the geometry (i.e. two-dimensional rotors with low *Ns*) and have a negative effect on performance.

Table 4: Variation of Gas Turbine Performance with Size (Tit = 1500.°K, Ns = .5)

P2/P1	T1	Tit			slip	Ns		etaT	Cp	Rg
3	293	1500			0.9	0.5		0.8	1005	286
RPM	omega	Delta H	U2	R2	Q	Pcomp	Eta-Comp	Eta-C(corr)	(GasTurb)	Eta(cycle)
		(m^2/s^2)	(m/sec)	(m)	(kg/sec)	(kW)			(kW)	
10,000	1047	135726	388	0.3708	11.3992	1547.169	0.85	0.80	2156.405	0.176
16,000	1676	137444	391	0.2332	4.5376	623.670	0.84	0.79	850.594	0.174
25,000	2618	139206	393	0.1502	1.8945	263.722	0.83	0.78	351.787	0.173
50,000	5236	141014	396	0.0756	0.4829	68.092	0.82	0.77	88.792	0.172
100,000	10472	142869	398	0.0380	0.1231	17.588	0.81	0.76	22.409	0.170
200,000	20944	129262	379	0.0181	0.0265	3.424	0.89	0.84	5.182	0.181
300,000	31416	150806	409	0.0130	0.0148	2.237	0.77	0.72	2.583	0.164
500,000	52360	155115	415	0.0079	0.0056	0.864	0.75	0.70	0.946	0.160
750,000	78540	162060	424	0.0054	0.0026	0.429	0.72	0.67	0.431	0.155
1,000,000	104720	169657	434	0.0041	0.0016	0.270	0.69	0.64	0.247	0.149
2,000,000	209439	178001	445	0.0021	0.0004	0.076	0.66	0.61	0.063	0.142
2,400,000	251327	187208	456	0.0018	0.0003	0.060	0.63	0.58	0.044	0.134

The extreme high *RPM* that are required together with the high temperatures, impose the use of oil free bearings. Pushing the air-bearings and electrical generators beyond the present limits is a challenging task.

The most advanced knowledge on small high temperature turbomachines is in the field of turbochargers, operating up to 200.000 RPM, and Auxiliary Power Units (APU). All operations above this limit require new developments as well in terms of material and manufacturing techniques as in terms of aero-thermodynamics [4]. There is also no guarantee that the existing flow solvers and turbulence models are still accurate also for these extremely low Reynolds numbers.

Previous study shows that the design of a small gas turbine with positive power output is a challenging task.

2.0 HEAT TRANSFER

Internal heat transfer has an important impact on the performance of the very small turbomachines, used in micro- and nano- gas turbines. The heat flux from the hot turbine to the colder compressor results in a cooling of the flow in the turbine and a heating of the flow in the compressor. The performance changes and can no longer be evaluated by the flow conditions measured at inlet and outlet of the components. This problem has first been recognized and studied for small turbochargers where it was shown that the distance between the hot turbine and the cold compressor might have a considerable impact on the flow conditions [5]. The impact on micro-turbomachinery performance has been discussed by Gong et al. [6] and Ribaud [7]. Procedures to correct for this internal heat transfer have been proposed [8].

2.1 Prediction Model

The diabatic compressor and turbine performance prediction is based on the assumption that the impeller friction losses are not changed by the heat transfer. However, heating the flow during the compression results in a higher outlet temperature, hence lower density at the compressor outlet. The main consequences are less diffusion than with adiabatic flow and, as can easily be evaluated from the outlet velocity triangles, lower work input and pressure rise. The latter ones result in a further decrease of the density at impeller outlet.

In what follows one will assume that the corresponding velocity increase at the outlet is compensated by a proportional increase of the impeller exit width. As a consequence the velocity is unchanged along the flow path. The original velocity triangles are re-established and friction losses can be evaluated from the polytropic efficiency of an adiabatic compression on an equivalent geometry. This can eventually be verified by a diabatic Navier-Stokes calculation.

Heating the flow during compression has a negative effect on the efficiency because the enthalpy *dh* needed for an elementary isentropic compression *dP* increases with the temperature.

$$dh = \frac{dP}{\rho} = \frac{dP}{P} R_G.T \tag{6}$$

Cooling the flow during the expansion in a turbine has also a negative effect on the efficiency because the energy *dh* obtained from an isentropic pressure drop *dP* decreases with decreasing temperature.

The first law of thermodynamics provides the relation for non isentropic diabatic compression:

$$dh = \frac{dP}{\rho} + TdS = \frac{dP}{\rho} + dL + dQ \tag{7}$$

where *dL* is the heat produced by the internal friction losses and *dQ* is the amount of heat transmitted trough the walls (Fig. 3).

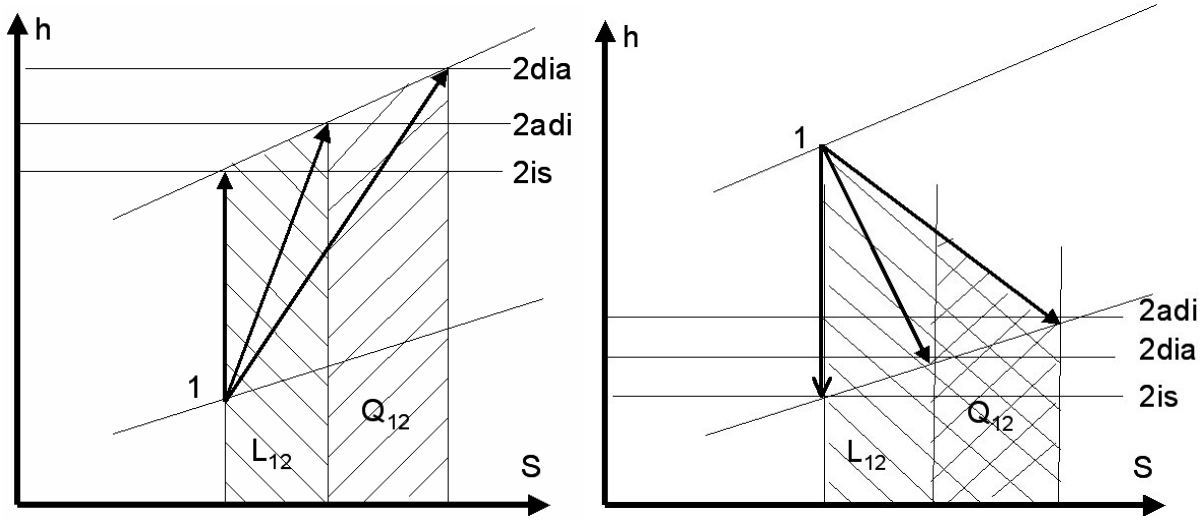

Figure 3: H,S Diagram for a Diabatic Compression (left) or Expansion (right).

Expressing the losses and heat addition as a linear function of the enthalpy rise

$$dL = \frac{L_{1,2}}{h_2 - h_1} dh \qquad dQ = \frac{Q_{1,2}}{h_2 - h_1} dh \tag{8}$$

and substituting it into (7) provides following relation.

$$\left(1 - \frac{L_{12}}{h_2 - h_1} - \frac{Q_{12}}{h_2 - h_1}\right) dh = \frac{dP}{\rho} \tag{9}$$

Using the relations for perfect gas to calculate the density and expressing the enthalpy in function of the temperature change and constant specific heat coefficient *Cp*, one obtains:

$$\left(1 - \frac{L_{12}}{Cp.(T_2 - T_1)} - \frac{Q_{12}}{Cp.(T_2 - T_1)}\right) dT = \frac{\gamma - 1}{\gamma} T \frac{dP}{P} \tag{10}$$

Integration from T_1 to T_2 (compressor) results in

$$\ln \frac{T_2}{T_1} \left(1 - \frac{L_{12} + Q_{12}}{Cp.(T_2 - T_1)}\right) = \frac{\gamma - 1}{\gamma} \ln \frac{P_2}{P_1} \tag{11}$$

or

$$\frac{T_2}{T_1} = \frac{P_2}{P_1}^{\mu} \tag{12}$$

where

$$\mu = \frac{\frac{\gamma - 1}{\gamma}}{1 - \frac{L_{12} + Q_{12}}{C_p.(T_2 - T_1)}} \tag{13}$$

Equation (12) is similar to the definition of polytropic efficiency of an adiabatic compression where μ stands for

$$\mu = \frac{\frac{\gamma - 1}{\gamma}}{\eta_p} \tag{14}$$

Hence

$$\eta_p = 1 - \frac{L_{12} + Q_{12}}{C_p.(T_2 - T_1)} \tag{15}$$

η_p decreases with positive values of Q_{12} because this increases both the nominator and denominator.

Equ. (15) shows that any heat addition will have the same effect as a reduction of polytropic efficiency. The value of L_{12} can directly be derived from (15) and the known polytropic efficiency for an adiabatic compression ($Q_{12}=0$).

$$L_{12} = \left(1 - \eta_{padi}\right) C_p.(T_{2adi} - T_1) \tag{16}$$

The same procedure provides the non adiabatic efficiency and outlet temperature T_{2dia} by substituting the previously defined value of L_{12} and a given value of $Q_{12} \neq 0$.

Similar equations are easily derived for turbines.

The diabatic outlet temperature ($Q_{12} \neq 0$) cannot directly be used to calculate the power transmitted by the compressor and turbine. The mechanical- or shaft power is obtained by subtracting the heat flux from the total energy transfer, defined by inlet and outlet temperature.

$$E_{C,dia} = \dot{m}.C_p(T_{2dia,comp} - T_1) - Q_{12} \qquad E_{T,dia} = \dot{m}.C_p(T_1 - T_{2dia,turb}) - Q_{12} \tag{17}$$

For a given pressure ratio, the real compressor and turbine efficiencies can also be defined from by substituting following corrected exit temperatures for compressor and turbine in (12):

$$T_{2,corr} = T_{2,dia} - Q_{12} / C_p / \dot{m} \qquad T_{2,corr} = T_{2,dia} + Q_{12} / C_p / \dot{m} \tag{18}$$

The decrease of efficiency of both components is shown on Fig. 4 and 5 as a function of adiabatic efficiency and Q_{12} between and turbine compressor. Q_{12} is expressed as a % of the adiabatic compressor power input at $\eta_p = .7$. It depends on the impeller size and fluid temperatures and is evaluated in next section.

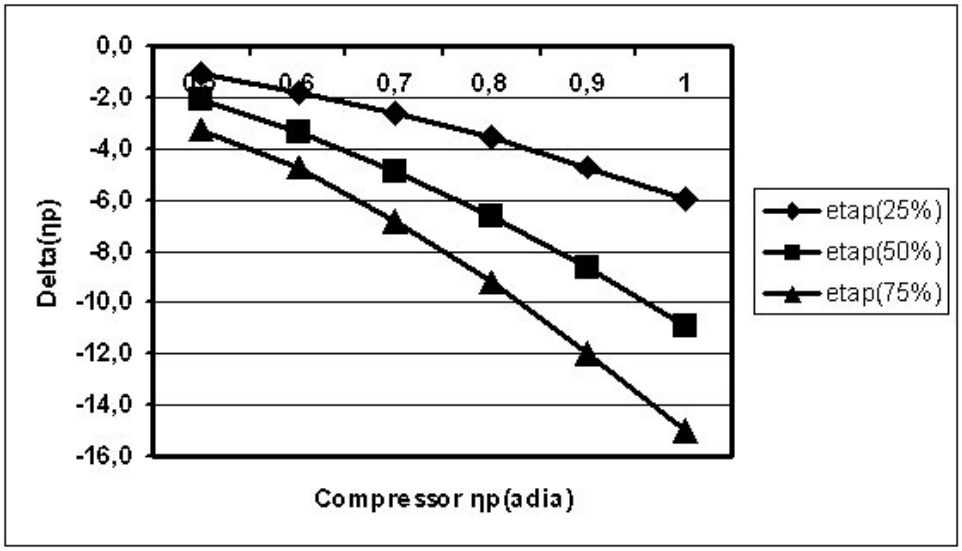

Figure 4: Decrease of Compressor Efficiency in Function of Q12 and η_p.

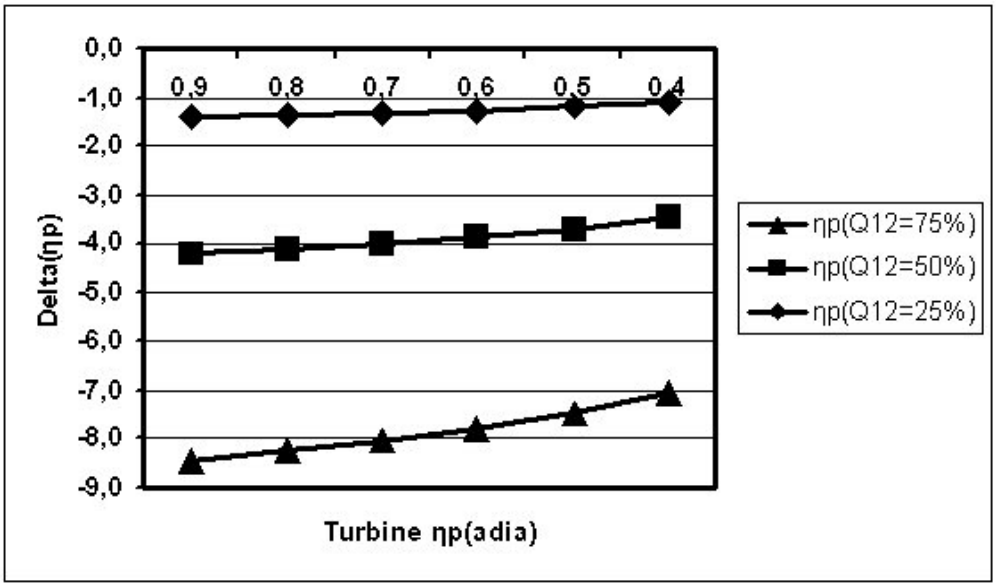

Figure 5: Decrease of Turbine Efficiency in Function of Q12 and η_p.

Input to this model is the internal heat transfer obtained from diabatic flow calculations on compressors of different size at different impeller surface temperatures.

2.2 Heat Flux Calculations

The amount of heat flux through the compressor walls ($Q_{12}>0$) depends on the compressor wall temperature which in turn is a function of the turbine inlet gas temperature, the blade and disk surface, the distance between turbine and compressor impeller, the conductivity of the material, the heat transfer coefficient, etc. A complete calculation requires a combination of a heat transfer calculation in the whole rotor with a diabatic flow calculation in the compressor and turbine (Fig. 6).

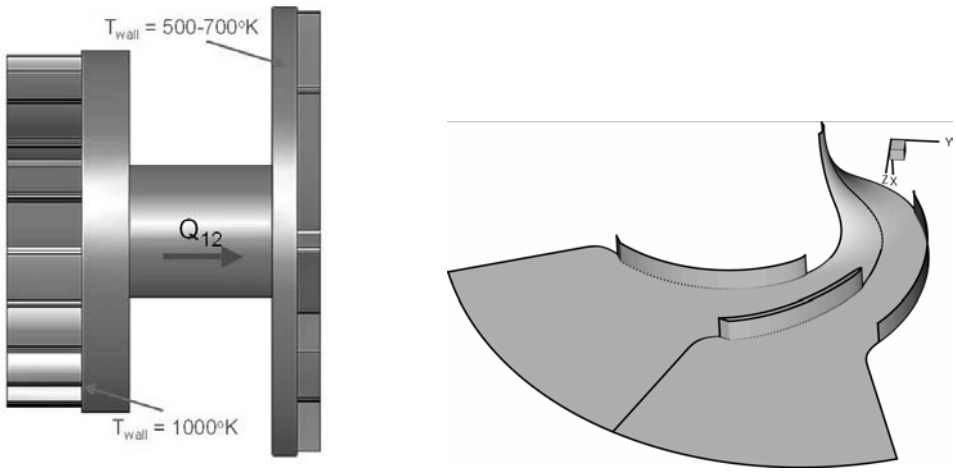

Figure 6: Rotor Geometry and View on Compressor Section.

Following is an estimation of typical values of the heat flux in radial compressor impellers of different size with different wall temperatures (Table 5). The flow and heat flux is calculated by the TRAF3D Navier Stokes solver developed by Arnone [9] on a grid with 400 000 cells using the Baldwin Lomax turbulence model. This may not be the most appropriate model but an experimental study of low Reynolds number flow in a rotating channel with wall roughness is presently under way to evaluate it.

Table 5: Navier Stokes Test Cases

Outlet diameter (mm)	8	20.
RPM	1050000	420000
Mass flow (gr/sec)	~1.	~6.7
P^0_2/P^0_1	2.1	2.1
T_{wall} (^{o}K)	600	500/600/700

The 20 mm diameter 2D compressor impeller is a geometrically scaled version of the 8 mm diameter one. It has four blades and four splitters (Fig. 6).

The model, explained in section 2, assumes the same velocity distribution inside the impeller for adiabatic and diabatic flows. Hence the inlet and outlet velocity triangles should be conserved during the diabatic calculations. This is achieved by:

- Adjusting the pressure ratio proportional to the inlet density ($dh=dP/\rho$) to obtain the same volume flow and hence the same inlet velocity triangles; and
- Increasing the impeller outlet width b_2 to compensate for the decrease in outlet flow density with increasing fluid temperature.

The heat flux is defined by integrating the flux on all surface cells (i.e. on the blades, hub and shroud). Fig. 7 shows the dependence of the calculated heat flux on compressor size and wall temperature. It varies between 27% of the large compressor power at 500 ^{o}K wall temperature to 62% at 700 ^{o}K wall temperature. It increases by almost 10% at the smaller impeller size.

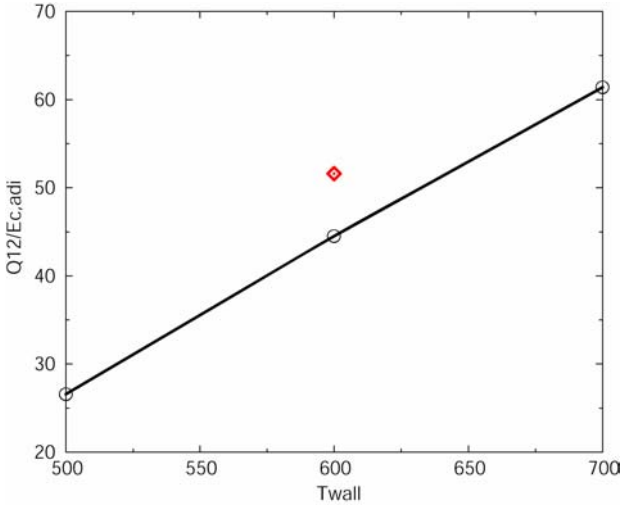

Figure 7: Variation of Heat Flux with Wall Temperature for 8 mm. Ø (◊) and 20 mm Ø (o) Impeller.

The Navier Stokes calculations predict a reduction of adiabatic impeller efficiency, based on shaft power and pressure ratio, from 69.6% to 63.5% for the diabatic compression. This value is in good agreement with the one defined by the analytical model.

2.3 Cycle Efficiency

The total energy needed for an adiabatic compression, or obtained from an adiabatic expansion from to P_2 to P_1 is

$$E_{C,adi} = \dot{m}C_p.(T_{2adi} - T_1) \qquad E_{T,adi} = \dot{m}C_p.(T_1 - T_{2adi}) \qquad (19)$$

The mechanical energy required to compress the gas in a diabatic process is defined in (17).

Although the adiabatic and diabatic compression processes suffer from the same friction losses, E_{dia} is larger than E_{adi} because the diabatic compression takes place at a higher temperature. For negative values of Q_{12} (cooling of the compressor) the required energy would be lower than the one specified in (19) because of the lower fluid temperature during compression. The process is then closer to the more efficient isothermal compression.

The opposite phenomenon occurs in the turbine. Expanding the flow in the turbine at a lower than adiabatic temperature, reduces the power output because the available energy, corresponding to a given pressure drop, decreases with decreasing temperature (6) $E_{T,adi} > E_{T,dia}$.

Heating the turbine would result in an increased power output in a way similar to what is expressed by the reheat factor for turbines.

Less power output from the turbine in combination with more power required by the compressor results in a lower gas turbine power output

$$E_{GT,dia} = E_{T,dia} - E_{C,dia} < E_{T,adi} - E_{C,adi} = E_{GT,adi} \qquad (20)$$

and lower cycle efficiency

$$\eta_{cycle} = \frac{E_T - E_C}{C_p \dot{m} (T_{iT} - C_{iT})} \tag{21}$$

C_{iT} is the combustion inlet temperature.

Following figures, showing the consequences for a typical small gas turbine rotor, are obtained at following operating conditions:

$P_2/P_1 = 3.$ $T_{1C}=293.\ ^oK$ $\eta_{pC} = .7$ $T_{It} = 1600.\ ^oK$ $\eta_{pT} = .8$

Fig. 8 shows the ratio of the diabatic over adiabatic power output as a function of the compressor polytropic efficiency for the typical cases of heat transfer. Q_{12} is 25.% 50.% or 75. % of the compressor adiabatic input power at polytropic efficiency of .7 . The central value is close to the 52% predicted in a micro gas turbine with rotor diameter 8 mm at 600 ^{o}K compressor wall temperature.

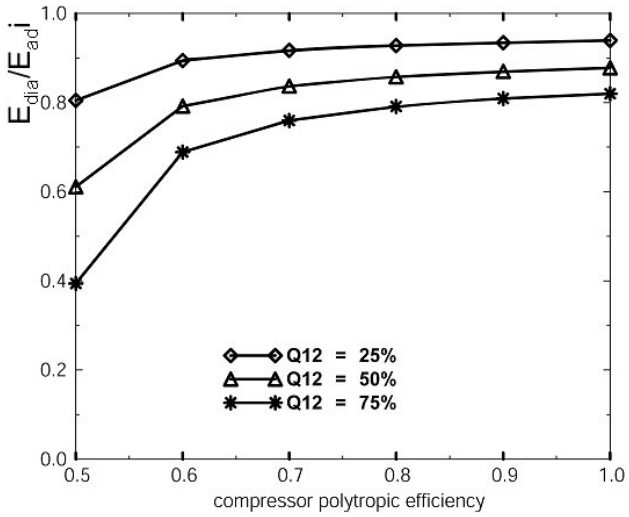

Figure 8: Ratio between Diabatic over Adiabatic Gas Turbine Power Output as Function of Compressor Polytropic Efficiency.

The heat-transfer from the turbine to the compressor as well as the lower compressor efficiency increase the compressor exit temperature and hence combustion chamber inlet temperature (Fig. 9). The effect is comparable to a recuperator and the corresponding increase of the combustion chamber inlet temperature means that less fuel will be needed to reach the prescribed turbine inlet temperature. This partially compensates the decreased compressor and turbine efficiency and explains the relatively small impact of the internal heat transfer on the cycle efficiency (Fig. 10).

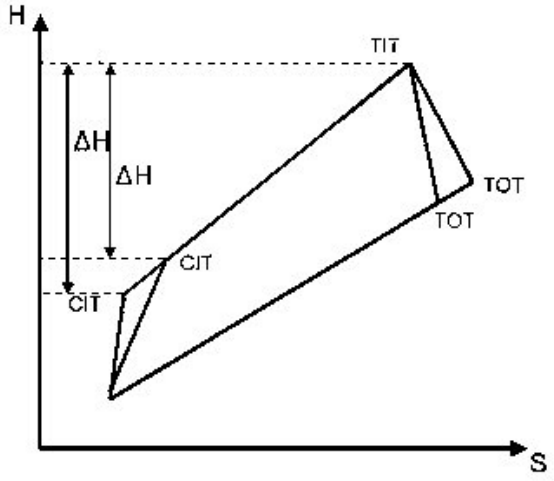

Figure 9: Effect of Internal Heat Transfer on Cycles (without recuperator).

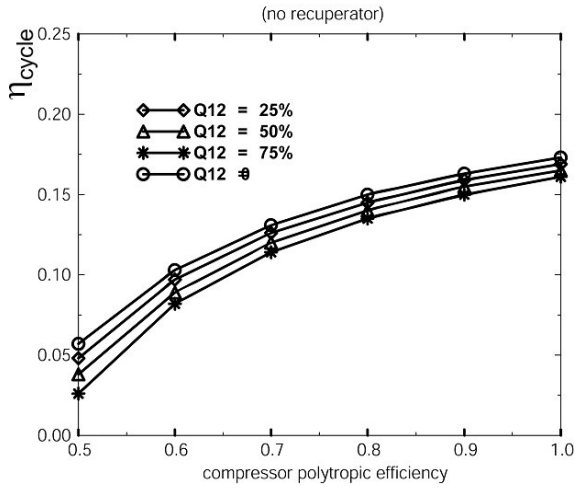

Figure 10: Effect of Internal Heat Transfer on Cycles (without recuperator).

This compensation does not occur if a recuperator is used (Fig. 11). The smaller difference between the turbine- and compressor exit temperature results in a smaller heat recuperation. Results shown on Fig. 12 indicate a non-negligible impact of heat transfer on cycle efficiency assuming a constant (.70) effectiveness of the recuperator.

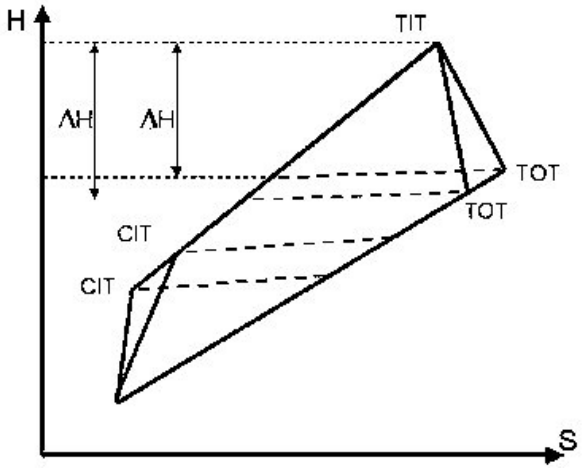

Figure 11: Effect of Internal Heat Transfer on Cycles (with recuperator).

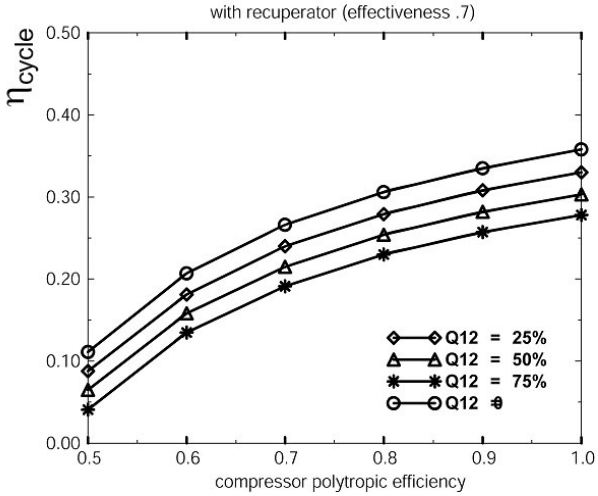

Figure 12: Impact of Heat Transfer on Cycle Efficiency (with recuperator).

3.0 CONSTRAINTS

Previous rules for turbomachinery scaling are valid only in combination with an exact geometrical scaling, i.e. scaling all dimensions, including blade thickness and roughness, with the same factor. This may not always be possible when going to extreme small dimensions. Limitations may occur depending on: different manufacturing techniques that are required to make the smaller geometries, new materials that are used or change of lay-out for operational or mechanical reasons.

Scaling the blade thickness proportional to the impeller diameter will lead to extreme thin blades that have an insufficient mechanical resistance to shocks or any other mechanical solicitations. Finite element calculations have also shown that a thickening of the blades and a larger fillet radius at the blade root may reduce stresses. However CFD evaluations show that a thickening the blades by a factor 4, as shown on Fig. 13, results in an efficiency drop of more than 6%.

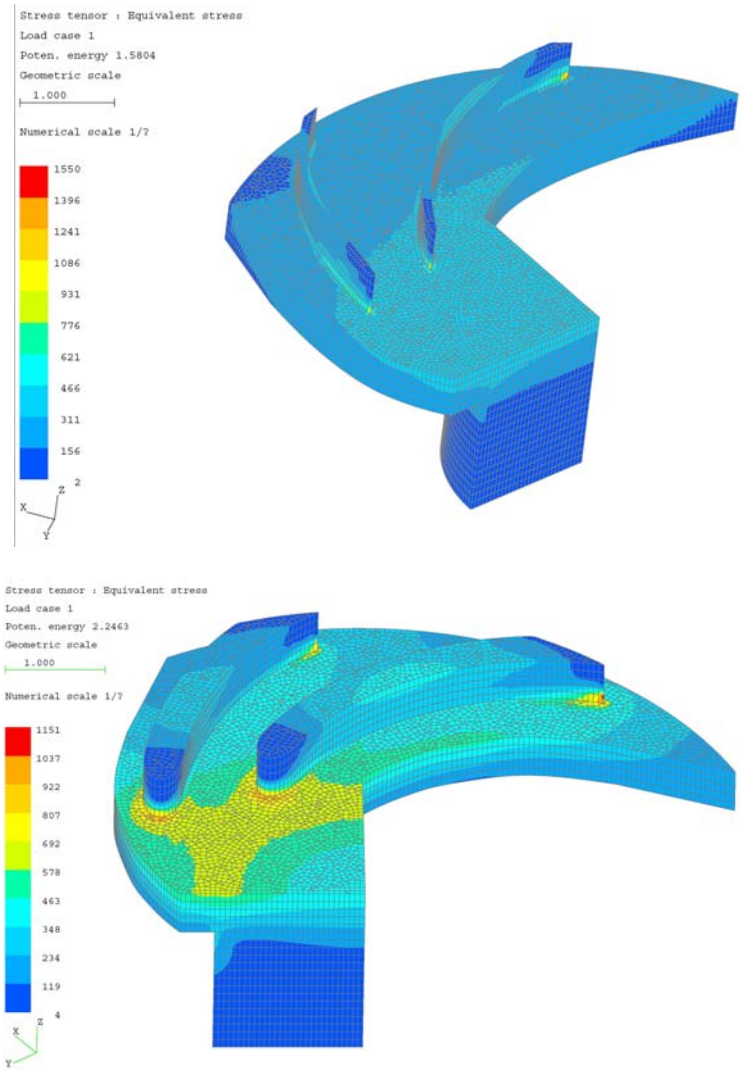

Figure 13: Effect of Blade Thickness on Stresses (different scales).

It is generally accepted that Roughness has no impact on friction losses as long as the Reynolds number based on the equivalent sand grain size *ks* is smaller than 100.

$$\mathrm{Re}_{ks} = \rho \frac{\omega . R_2 . ks}{\mu} < 100 \qquad (22)$$

The etching techniques, used for nano-gas turbine rotors, do not allow very smooth surfaces which may limit the validity of Reynolds number influence on efficiency (Fig. 1). It is further not verified that this rule of thumb (22) is still valid for the very low Reynolds numbers.

The decrease in efficiency with decreasing size requires higher peripheral velocities at impeller exit to reach the required pressure ratio. Hence the stress problems increase at reduced dimensions. It has been shown that shrouding the impellers has a favourable impact on the blade bending stresses but results in high stresses at the shroud eye (Fig. 14).

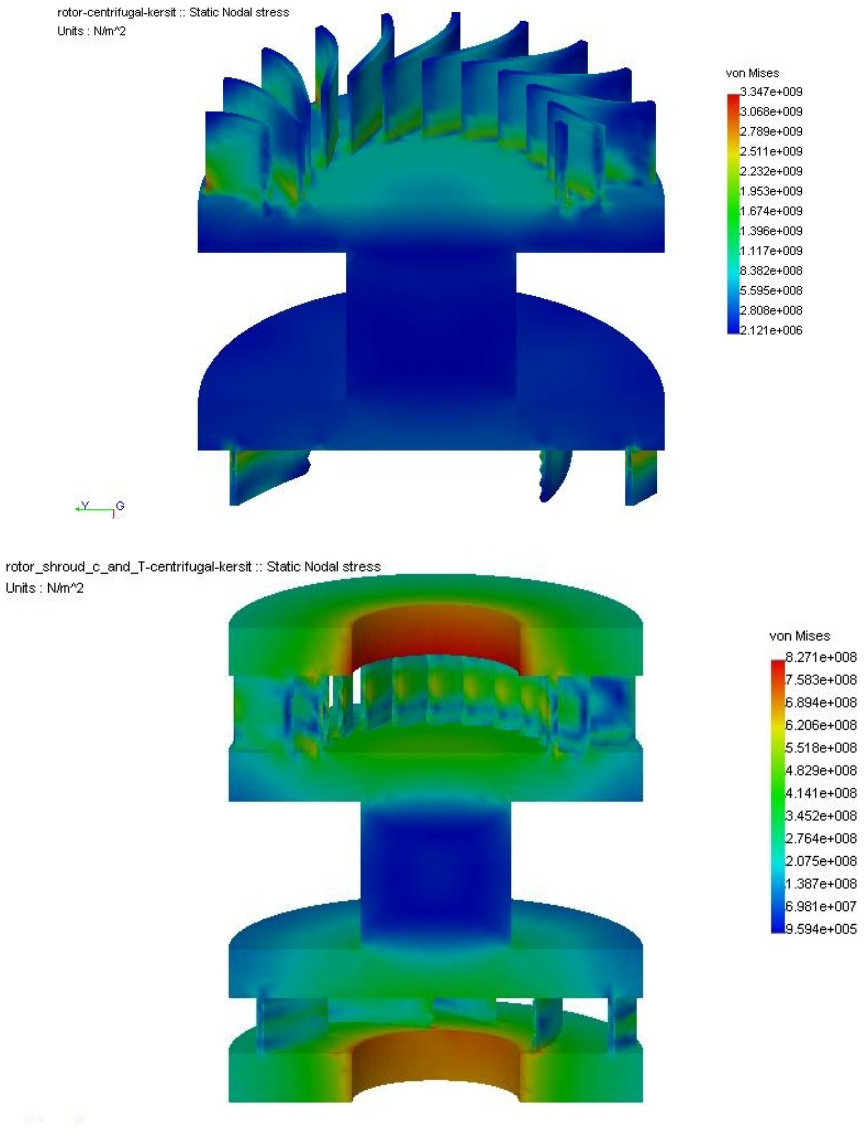

Figure 14: von Mises Stresses in Unshrouded and Shrouded Impeller.

Adding a shroud to the impeller has a small favourable effect on efficiency. The friction of the fluid on the non-rotating shroud wall (with velocity V) and the losses by the clearance flow, are replaced by a friction of the fluid on the rotating shroud (with velocity W) and friction on the rotating shroud wall (with velocity U) (Fig. 15). The net effect is a small increase of efficiency of the order of 1 to 2% depending on the thickness of the outer rim.

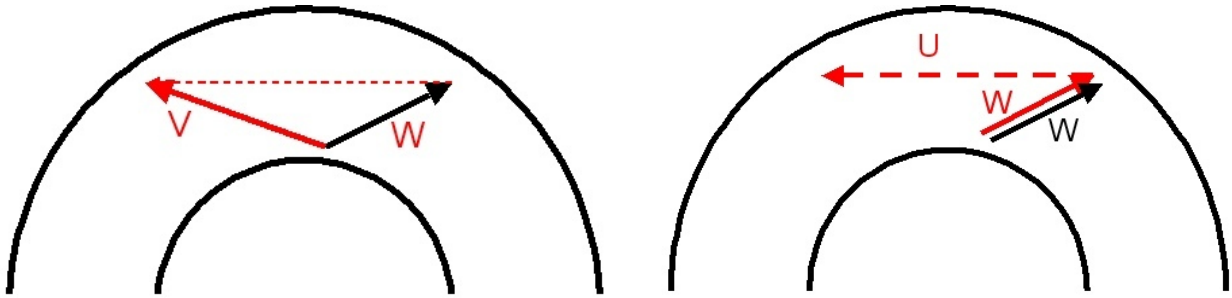

Figure 15: Friction on Unshrouded (left) and Shrouded (right) Impeller.

One of the micro gas turbine design targets is a compact machine with high power density. Integrating the rotor of the electrical power generator into the compressor shroud may help to reach this goal. It also alleviates vibration problems resulting from long rotors.

4.0 CONCLUSIONS

Good micro gas turbines are not miniaturized copies of large ones.

- The non-adiabatic compression and expansion perturbs the whole thermodynamic cycle.
- Combustion chambers, not yet discussed in this paper, are very different from their larger version because of unscalable characteristics like combustion time.

The very high rotational speed, that is needed to obtain the enthalpy and pressure changes prescribed by the gas turbine cycle, is the major mechanical problem.

New materials and new manufacturing techniques are needed. They should allow low cost production because this small power output devises remain in competition with heavier but cheap batteries.

One of the major problems in micro gas turbines is the decrease of compressor and turbine efficiency with decreasing dimensions. This is further enhanced by the effect of larger roughness resulting from materials and manufacturing techniques. The resulting decrease in cycle efficiency does not make micro gas turbines to ecological devices. Performance more than any other criterion might define the lower limit for these devises.

ACKNOWLEDGMENT

Part of the results presented in this lecture are obtained in the context of the project SBO 030288 “PowerMEMS” financed by IWT (Institute for Promotion and Innovation of Science and Technology in Flanders).

The contribution by Z. Alsalihi and T. Verstraete to this lecture is gratefully acknowledged.

REFERENCES

[1] Japikse D. and Baynes N., Introduction to Turbomachines, Concepts ETI and Oxford University Press, 1994.

[2] Rodgers C., Specific Speed and Efficiency of Centrifugal Impellers, proc. ASME 25th Gas Turbine Conference, 1980.

[3] Van den Braembussche R.A., Islek A.A. and Alsalihi Z., Aero-thermal Optimization of Micro-Gas Turbine Compressors Including Heat Transfer, Proceedings of the IGTC2003Tokyo, International Gas Turbine Conference 2003, Tokyo, November 2-7, 2003.

[4] Nagashima T., Ribaud Y., Ivanov M.J. and Van den Braembussche R.A., Collaborative Research about Thermo- Fluid-dynamic Design of Ultra –micro Gas Turbine, Journal of the Gas Turbine Society of Japan, Vol. 30, No 4, 2002, pp. 42-49.

[5] Rautenberg M., Mobarak A. and Malobabic M., "Influence of Heat Transfer between Turbine and Compressor on the Performance of small Turbochargers", GTSJ Intl. Gas Turbine Congress, Tokyo, 23-29 November, 1983.

[6] Gong Y., Sirakov B.T., Epstein A.H and Tan C.S., "Aerothermodynamics of micro-turbomachinery", ASME-GT2004-53877.

[7] Ribaud Y., "Internal Heat Mixing and External Heat losses in an Ultra Micro Turbine" Proceedings International Gas Turbine Congress 2003 Tokyo, November 2-7, 2003. IGTC2003Tokyo OS-109.

[8] Rautenberg M. and Kammer N., "On the thermodynamics of non-adiabatic compression and Expansion Processes in Turbomachines", 5th Intl. Conference for Mechanical Power Engineering, October 13-15, 1984.

[9] Arnone A., "Viscous analysis of Three-Dimensional Rotor Flow Using a Multigrid Method" ASME Journal of Turbomachinery, Vol. 116.